IEEE Photonics Journal
An IEEE Photonics Society Publication

Open Access

Experimental Comparison of PAM, CAP, and DMT Modulations in Phosphorescent White LED Transmission Link

Volume 7, Number 3, June 2015

G. Stepniak
L. Maksymiuk
J. Siuzdak, Member, IEEE

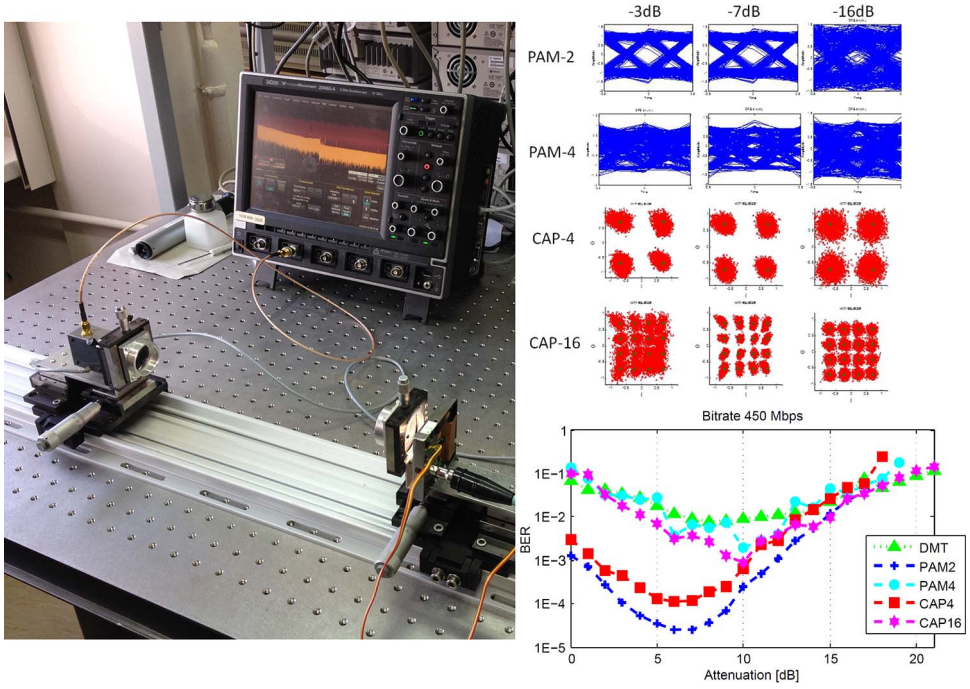

DOI: 10.1109/JPHOT.2015.2427092
1943-0655 © 2015 IEEE

IEEE photonics SOCIETY

IEEE

Experimental Comparison of PAM, CAP, and DMT Modulations in Phosphorescent White LED Transmission Link

G. Stepniak, L. Maksymiuk, and J. Siuzdak, *Member, IEEE*

Institute of Telecommunications, Warsaw University of Technology, 00-665 Warsaw, Poland

DOI: 10.1109/JPHOT.2015.2427092

Manuscript received March 31, 2015; revised April 22, 2015; accepted April 22, 2015. Date of publication April 28, 2015; date of current version May 19, 2015. This work was supported by the Polish National Science Center under Grant 2011/03/B/ST7/00204. Corresponding author: G. Stepniak (e-mail: stepniak@tele.pw.edu.pl).

Abstract: In the paper, an experimental comparison of pulse amplitude, carrierless amplitude–phase, and discrete multitone modulations is carried in a visible light communications link employing white phosphorescent light-emitting diode (LED) as a transmitter. By changing the modulation index, the influence of LED nonlinearity on the performance is studied. The results indicate similar performance of pulse-amplitude modulation (PAM) and carrier-less amplitude–phase (CAP) (with a slight advantage of the former) and substantially worse performance of DMT.

Index Terms: Visible light communications, light-emitting diodes.

1. Introduction

Visible light communications (VLC) with use of white lighting light emitting diodes (LED) as transmitters is considered an attractive alternative to radio transmission in personal communications or within the pico-cells of the 5G mobile standard [1]–[3]. Among different lighting LEDs, the cheapest and most popular are chips emitting blue light covered with a phosphorescent layer, that converts the blue light into yellow component, which together with the blue one generates white spectrum. The process of yellow light generation at the phosphorescent layer has a substantially higher time constant than the chip itself and hence a blue filter is typically used at the receiver to eliminate this slow component and reduce the inter-symbol interference (ISI). However, the level of ISI even with the blue filter remains high, and advanced modulation formats with aid of a serious amount of digital signal processing (DSP) are needed to achieve competitive bit rates. Usually, three modulation formats of the highest efficiency in direct-detection short-reach links are considered, namely, pulse amplitude modulation (PAM), carrier-less amplitude–phase (CAP) and discrete multitone (DMT). In all cases, data rates in excess of 1 Gbit/s has been achieved under typical intra-office lighting conditions [4]–[6]. However, according to our knowledge, those three modulations have never been directly compared at the same experimental conditions, with a phosphorescent white LED acting as a transmitter. In this paper, we aim at filling this gap. So far, similar studies have been carried out in polymer optical fibers (POF) [7]–[9], and also for RGB lighting LED [10], with the conclusion that DMT is considerably less efficient than PAM or CAP, which present a comparable performance. However, due to severe nonlinearity of the LED, this comparison is more difficult in the VLC link and must be

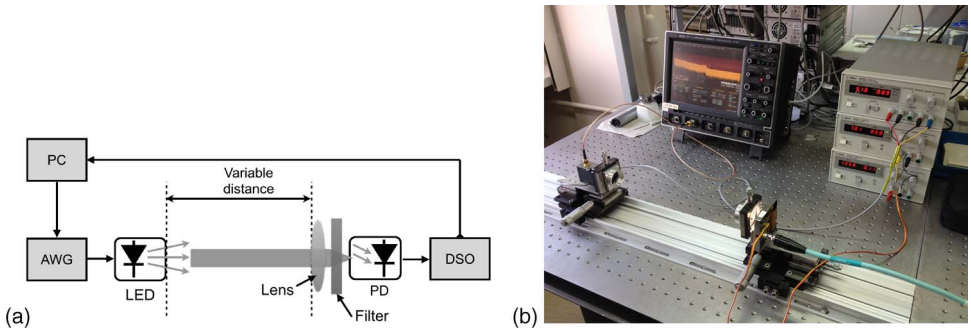

Fig. 1. (a) Diagram of the experimental set up. (b) Detail of the test object used.

done for various levels of the modulation index. The nonlinear behavior of LEDs output power as a function of modulating current is a well-known phenomenon, which is caused mostly by thermal effects. A higher modulating current increases the junction temperature and decreases the efficiency of electrical to optical conversion efficiency [11].

We restrict our analysis to a case, where neither polynomial precompensation nor nonlinearity counteracting algorithms are employed (like Volterra Equalizer for CAP or PAM [12], or different methods for DMT [13]). The efficiency of these should be a subject of a further study. The paper is organized as follows. First, we describe the experimental setup, then we outline the generation and reception of different modulation formats. Finally, we show the experimental results and discuss them.

2. Experimental Setup

A block scheme of the experimental setup is shown in Fig. 1(a), and a photograph of it is shown in Fig. 1(b). The signal of different modulations was first generated offline by a Matlab program and uploaded to the memory of the arbitrary waveform generator (AWG), which in turn modulated a commercially available visible light (Osram LE UW Q9WP-single LED source) LED via a specially designed driving circuit. The LED was biased at 500 mA as for this value the best performance was observed. The amplitude of the signal, which modulated the LED was set using external coaxial attenuators. The modulation index defined as $\mathrm{MI} = (I_{\max} - I_{\min})/(I_{\max} + I_{\min})$ changed in the range from below 20% to 100% for 16 to 0 dB of external attenuation, respectively. Obviously, for the highest indices analog clipping of the signal was present. The photo receiver (p-i-n photodiode Hamamatsu S5972 of 0.8 mm diameter connected to the transimpedance amplifier TIA MAX3665) was equipped with a convex lens of 3 cm diameter and 40 mm focal length, and an optical low pass filter with cutoff wavelength at 480 nm to suppress the low-speed light component generated by the phosphor layer. The distance from the LED to the lens was 30 cm, which corresponded to the luminous flux at the lens aperture of 750 Lux. The received signal was fed to digital sampling oscilloscope (LeCroy 204MXi), recorded there, and the further processing took place off line [see Fig. 1(a)]. We decided to study two bitrates: 300 Mbit/s and 450 Mbit/s, which were well below the capabilities of the setup (which allowed for above 1 Gbit/s transmission [6]), but provided a sufficient power margin to conduct a fair comparison of the schemes. A comparison at higher bit rates (e.g., 600 Mbit/s) would require increasing the illumination level.

To compare different modulations, two signal amplitude normalization methods are possible. In the first one, the amplitudes of the signals are normalized to their peak values, which results in different signal powers, depending on their peak to average power ratios (PAPR). In the second one, which was applied here, the (electrical) powers of all the modulating signals are equal. This results in different peak amplitudes for different modulations. As the PAPR is the highest for DMT, its amplitude was set to unity and amplitudes of signals of the remaining modulation formats were reduced to have the same (electrical) power as the DMT signal. The amplitude coefficients were set both at the AWG and using external attenuators.

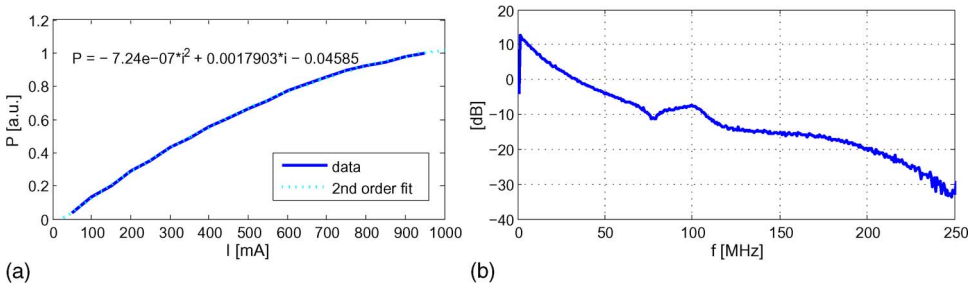

Fig. 2. (a) LED output power versus bias current with the fitted second-order polynomial. (b) Frequency response of the link measured for 500 mA bias current.

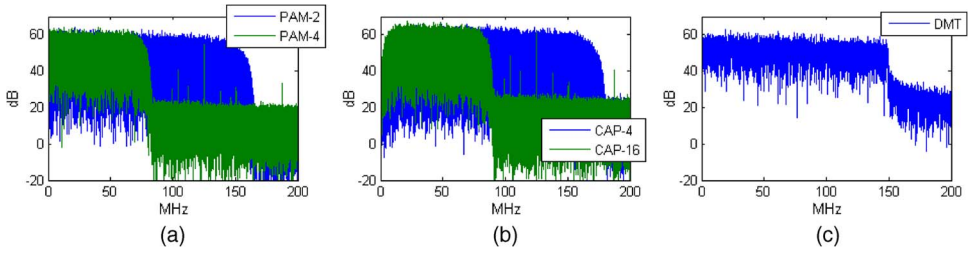

Fig. 3. Spectra of transmitted signal of different modulations for 300 Mbit/s. (a) PAM. (b) CAP. (c) DMT.

The frequency response of the setup [shown in Fig. 2(b)] exhibits the 3 dB bandwidth (with blue filter) of 12 MHz. The static nonlinearity characteristics of the transmitter was measured for variable bias current [shown in Fig. 2(a)] is typical for lighting LEDs (e.g., [14, Fig. 2] and [15, Fig. 2]).

2.1 Pulse Amplitude Modulation

The PAM signal consisted of 100 k randomly generated symbols with two or four amplitude levels (for PAM-2 and PAM-4, respectively). The symbols were oversampled with a factor of 2 to subsequently perform root raised cosine (RRC) filtering [16], where the roll-off parameter of the filter was $\alpha = 0.2$. The spectrum of PAM is shown in Fig. 3(a). After transmission, the signal from the oscilloscope was resampled and filtered with the transmitter matched filter. Next, downsampling and symbol-spaced decision feedback equalization (DFE) took place. The equalizer had 30 feed forward and 10 backward taps and the recursive least squares (RLS) algorithm has been used for adaptation of its coefficients. The first 1500 symbols of the data signal were used for the training sequence. Finally, error vector magnitude (EVM) and bit error rate (BER) were calculated.

2.2 Carrierless Amplitude–Phase

The CAP signal consisted of 50k symbols with two and four amplitude levels, which taking into account that CAP is a 2-dimensional scheme corresponds to CAP-4 and CAP-16. The symbols were mapped into the inphase and quadrature components, upsampled with a factor of 4 and convolved with the transmission filters, which are [16]

$$g_i(t) = g(t)\cos\left(2\pi f_s \frac{1+\alpha}{2} t\right) \tag{1}$$

and

$$g_q(t) = g(t)\sin\left(2\pi f_s \frac{1+\alpha}{2} t\right) \tag{2}$$

for the inphase and quadrature components, respectively, and where $g(t)$ is the RRC filter having roll-off factor α. The baud rate (f_s) for CAP signal was half of the PAM baud rate so that the

throughput of both modulations with the same level number was equal. The spectrum of CAP is shown in Fig. 3(b). Due to the shift towards higher frequencies (for $\alpha > 0$) the CAP signal occupies higher bandwidth than corresponding PAM signal of the same roll-off, number of levels and bit rate. After transmission the signal was resampled, filtered with transceiver filters and downsampled to the symbol rate. The DFE, its convergence algorithm and training sequence length was the same as in PAM case, with the only difference that now it is a complex equalizer (with 2×4 filters) [17].

2.3 Discrete Multitone

DMT is a variant of orthogonal frequency division multiplexing (OFDM), which applies Hermitian symmetry to the transmitted symbols to yield a real-valued time-domain signal and hence is well suited to low-pass channels such as VLC. The DMT signal in the experiment consisted of 126 subcarriers (and the FFT size of 256), and the length of the cyclic prefix (CP) was 30 samples. The number of DMT symbols was 2000 to ensure roughly the same data volume as in the two previous modulations. The clipping level was set at the level of about 11 dB, which is typical for this modulation [7]. A single tap phase/amplitude equalizer was used at the receiver to follow the constellation rotation due to the lack of the synchronization between the transmitter and receiver. After the initial training over 50 symbols this equalizer operated in decision-directed mode. The frequency of the highest subcarrier was 150 MHz regardless the bitrate. Fig. 3(c) shows example spectrum of a DMT signal with even powers of all subcarriers. Before the actual transmission, EVM and SNR for different subcarriers were estimated using a training signal having all subcarriers loaded with quadrature amplitude modulation (QAM-4). Next, the bit and power loading has been done using a slightly modified Fischer's algorithm [18]. This procedure, given the target bit rate and SNR in the subcarriers, loads the bits to minimize the BER. Although the BER can be estimated directly from the algorithm, the signal with the new bit and power loading was generated once again and transmitted for verification. Example bit and power loading along with the measured BER and constellations are shown for 300 Mbit/s transmission in Fig. 4.

3. Results and Discussion

The comparison of modulations BER performance vs. bit rate for 300 Mbit/s is shown in Fig. 5. The BER behavior is typical for a system with nonlinearities. For high signal powers (low attenuation) the nonlinearity is the primary cause of signal distortion. Thus, when attenuation is increased, the nonlinearity influence is relaxed and BER decreases for any modulation. However, if the signal power is decreased too much, the noise influence increases and BER rises again. The results can be analyzed in two different regions. In the first one, the performance is limited by nonlinear distortions. This region extends for the attenuation range of 0–7 dB for 2 level PAM and CAP and for approximately 0–10 dB for 4 level PAM and CAP and DMT. The second region (linear region) is for respectively higher attenuation values and here the dominating source of interference is the receiver noise. At the intersection of the two regions all the modulations exhibit minimum BER. This behavior is also confirmed in the eye and constellation diagrams, which are shown in Fig. 6 for three different attenuation levels. For 3 dB attenuation a significant amount of nonlinear distortions is observed, which manifests by asymmetry and unequal spacing between the amplitude levels for PAM-4. In CAP, the symbols with higher distance from the constellation center are more distorted, and as the P-I curve has a different slope for low and high currents, asymmetry of the distortion is also visible. For 16 dB attenuation, the diagrams are distorted mostly by the noise. For 7 dB attenuation (corresponding to the MI of app. 58%) the diagrams show performance close to optimum. It should also be noted that received power at minimum BER for PAM-2 and CAP-4 was higher than for the remaining modulations (as it corresponded to a lower attenuation), which also explains their better performance. These results confirm a quite intuitive fact that 2 level modulations are more immune to nonlinearity then modulations with higher number of levels. The optimum attenuation level for DMT was similar as for

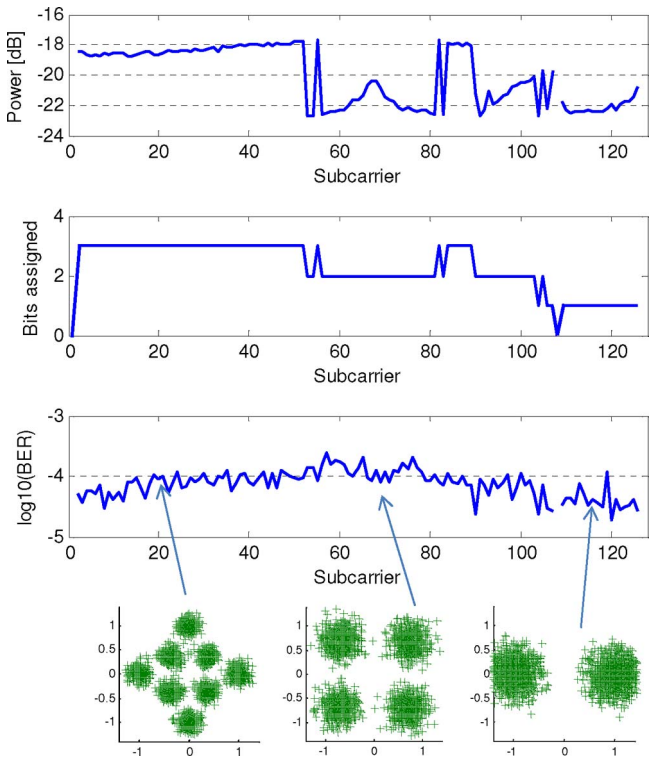

Fig. 4. Power loading, bit assignment, and BER vs. subcarrier number and exemplary received constellations for 300 Mbit/s DMT transmission with 7 dB attenuation.

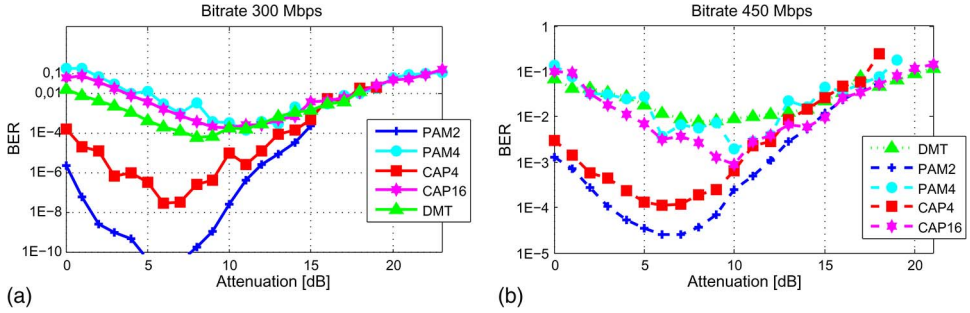

Fig. 5. BER vs. modulating signal attenuation for 300 Mbit/s (a) and 450 Mbit/s (b).

CAP-16 and PAM-4. This also suggests a lower immunity of multicarrier modulations to nonlinearity. The second conclusion from Fig. 5 is that the 2-level modulations performed better than the 4-level. Obviously, this is partially caused by the mentioned immunity to nonlinearity and could be reversed for higher bit rates, where the equalization penalty might dominate over the multi-level penalty. At some point, this happens for 450 Mbit/s [see Fig. 5(b)] in the linear range. Based on these two figures, we can also conclude that PAM-2 performance was clearly better than CAP-4, although CAP-16 and PAM-4 behaved quite similar (with a slight advantage of CAP-16). Finally, the DMT performance was substantially worse than the performance of 2-level modulations.

The influence of nonlinearity on the DMT modulation is readily seen in Fig. 7, where values of signal to interference + noise ratio (SINR) are calculated based on EVM for each subchannel. For a high attenuation (e.g., 16 dB), the power of the DMT signal is the least, and the system performance is limited by receiver noise, and the SINR approximately follows the frequency response of the link [shown in Fig. 2(b)]. For a low attenuation (e.g., 3 dB), the power of the signal

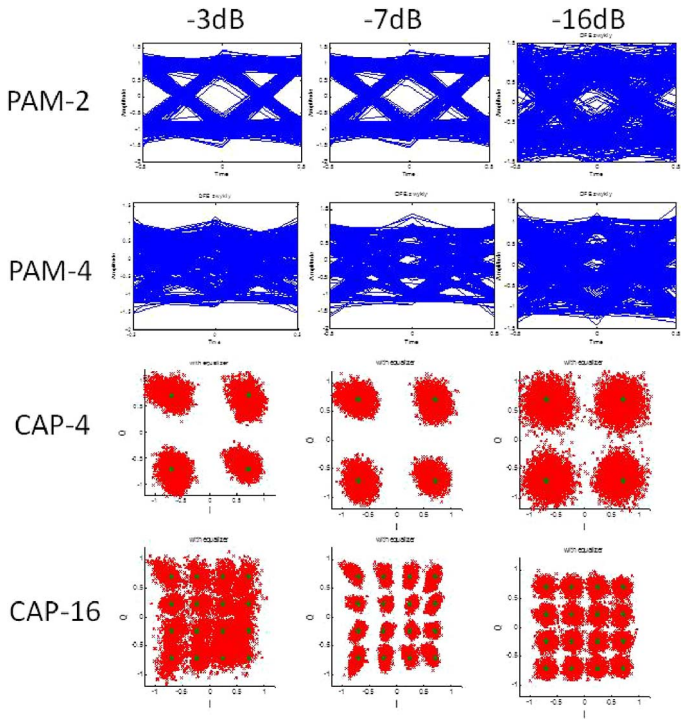

Fig. 6. PAM eye-diagrams and CAP constellations for three different attenuation.

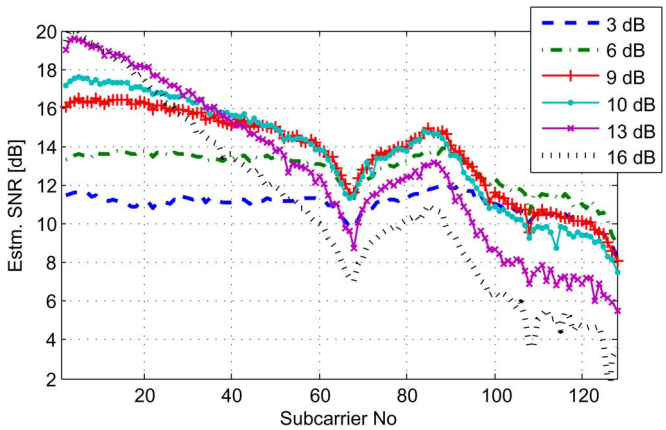

Fig. 7. Estimated SINR versus DMT subcarrier number for various attenuator levels [dB] (given in the legend) and 300 Mbit/s transmission.

is the greatest, which reduces SINR for low frequency channels due to nonlinearity. However, the high frequency channels SINR is boosted, as the increase of the signal power prevails over the nonlinear distortion. This is because of the low signal power for these channels. In effect, for high signal power (low attenuation) the value of SINR is roughly the same for all channels, except for those close to the cut off frequency.

The worse performance of DMT in the presence of non-linear distortions as compared to 2-level PAM ad CAP modulations may be explained by studying their amplitude probability density functions (PDF). If we consider the static nonlinearity only [see Fig. 2(a)], the powers of second, third and higher order distortions are given by higher order moments of the modulating signal, i.e., $m_4 = E(x^4)$, $m_6 = E(x^6)$ for the second- and third-order distortions, respectively.

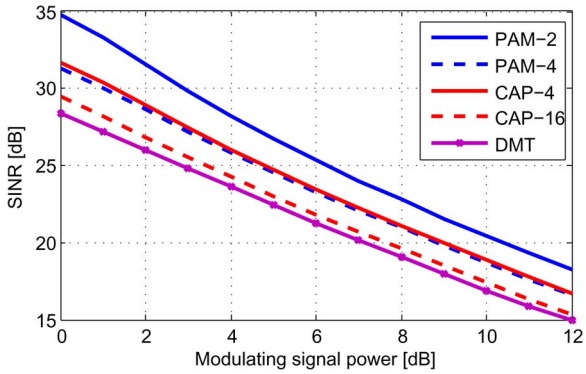

Fig. 8. SINR versus modulating signal power. Power of 0 dB corresponds to PAM-2 with reference peak-peak amplitude of $I_{ref} = 150$ mA (or $I_{ref} \times \gamma_{mod}/\gamma_{pam}$ for the remaining modulations).

The DMT modulation has a Gaussian PDF, and therefore, it has greater values of high order moments, thus it generates higher levels of nonlinear distortions. The CAP and PAM PDFs are more compact and therefore they generate lower levels of nonlinear distortions.

To validate this theory, we performed careful calculations of SINR, taking into account actual PDFs of the modulations and the static nonlinearity shown in Fig. 2(a). If there is no additive noise in the system, the SINR can be defined as

$$\text{SINR} = \frac{P_{\text{lin}}}{P_{n\text{lin}}} \tag{3}$$

where the power of useful signal is

$$P_{\text{lin}} = \int_{-\infty}^{\infty} a^2 (x - x_{\text{bias}})^2 pdf(x) dx \tag{4}$$

and where a is the slope of the P-I curve $f(x)$ at x_{bias}, and $pdf(x)$ is the amplitude probability density function of the modulation. It is noted that modulation PDFs are symmetrical against 0. In a similar way, the power of the nonlinear distortion is

$$P_{nlin} = \int_{-\infty}^{\infty} (f(x - x_{bias}) - a(x - x_{bias}))^2 pdf(x) dx. \tag{5}$$

PDFs of different modulations were derived analytically [19]. The results indicate that for the same modulating power, the SINR for DMT is 3–5 dB lower than for PAM-2 (see Fig. 8). This figure also explains the worse operation of 4-level modulations, although based on this theoretical calculation of SINR a bit better operation of PAM-4 could be expected in the experiment. Finally, CAP-4 and PAM-4 exhibit similar SINR for the same signal power level (see Fig. 8). However, as it comes to BER, CAP-4 is much better as its constellation points are further apart than in PAM-4.

4. Conclusion

In this paper we have experimentally compared three advanced modulation formats in a transmission link employing a white lighting LED with phosphorescent layer. As the LED introduces a significant level of nonlinear distortions, the performance was compared as a function of the modulating index, whereas in a fairly linear link such as POF [7]–[9], the power efficiency of a modulation (low PAPR) is the key factor, in the VLC link studied in this paper, it is the immunity to nonlinear distortions that determines the final performance. The results indicate that 2-level PAM and CAP modulations exhibit better immunity to nonlinear distortions and allow for lower

BER than their 4-level counterparts. The operation of PAM-4 and CAP-16 was similar to DMT. The lowest BER was achieved with PAM-2.

Acknowledgment

Part of the laboratory equipment used in this paper was funded in the framework of the EU Innovative Economy FOTEH project.

References

[1] J. Grubor, S. Randel, K.-D. Langer, and J. Walewski, "Broadband information broadcasting using LED-based interior lighting," *J. Lightw. Technol.*, vol. 26, no. 24, pp. 3883–3892, Dec. 2008.
[2] H. Elgala, R. Mesleh, and H. Haas, "Indoor optical wireless communication: Potential and state-of-the-art," *IEEE Commun. Mag.*, vol. 49, no. 24, pp. 56–62, Sep. 2011.
[3] H. Haas, "Visible light communications," in *Proc. OFC/NFOEC*, paper Tu2G.5.
[4] A. Khalid, G. Cossu, R. Corsini, P. Choudhury, and E. Ciaramella, "1-Gb/s transmission over a phosphorescent white LED by using rate-adaptive discrete multitone modulation," *IEEE Photon. J.*, vol. 4, pp. 1465–1473, Oct. 2012.
[5] F.-M. Wu *et al.*, "1.1 Gb/s white-LED-based communication employing carrier-less amplitude and phase modulation," *IEEE Photon. Technol. Lett.*, vol. 24, no. 19, pp. 1730–1732, Oct. 2012.
[6] G. Stepniak, L. Maksymiuk, and J. Siuzdak, "1.1 Gbit/s white lighting LED based visible light link with pulse amplitude modulation and Volterra DFE equalization," *Microw. Opt. Technol. Lett.*, vol. 5, no. 7, pp. 1620–1622, 2015.
[7] S. Randel, F. Breyer, S. Lee, and J. Walewski, "Advanced modulation schemes for short-range optical communications," *IEEE J. Sel. Topics Quantum Electron.*, vol. 16, no. 5, pp. 1280–1289, Sep./Oct. 2010.
[8] G. Stepniak and J. Siuzdak, "Experimental investigation of PAM, CAP and DMT modulations efficiency over a double-step-index polymer optical fiber," *Opt. Fiber Technol.*, vol. 20, no. 4, pp. 369–373, Aug. 2014.
[9] S. Loquai *et al.*, "Comparison of modulation schemes for 10.7 Gb/s transmission over large-core 1 mm PMMA polymer optical fiber," *J. Lightw. Technol.*, vol. 31, no. 13, pp. 2170–2176, Jul. 2013.
[10] F. Wu *et al.*, "Performance comparison of OFDM signal and CAP signal over high capacity RGB-LED-based WDM visible light communication," *IEEE Photon. J.*, vol. 5, no. 4, Aug. 2013.
[11] E. Schubert, *Light-Emitting Diodes*. Cambridge, U.K.: Cambridge Univ. Press, 2006.
[12] G. Stepniak, J. Siuzdak, and P. Zwierko, "Compensation of a VLC phosphorescent white LED nonlinearity by means of Volterra DFE," *IEEE Photon. Technol. Lett.*, vol. 25, no. 16, pp. 1597–1600, Aug. 2013.
[13] R. Mesleh, H. Elgala, and H. Haas, "LED nonlinearity mitigation techniques in optical wireless OFDM communication systems," *J. Opt. Commun. Netw.*, vol. 4, no. 11, pp. 865–875, Nov. 2012.
[14] J. Li, Z. Huang, X. Liu, and Y. Ji, "Hybrid time–frequency domain equalization for LED nonlinearity mitigation in OFDM-based VLC systems," *Opt. Exp.*, vol. 23, no. 1, pp. 611–619, 2015.
[15] I. Neokosmidis, T. Kamalakis, J. W. Walewski, B. Inan, and T. Sphicopoulos, "Impact of nonlinear LED transfer function on discrete multitone modulation: analytical approach," *J. Lightw. Technol.*, vol. 27, no. 22, pp. 4970–4978, Nov. 2009.
[16] J. J. Werner, "Tutorial on carrierless AM/PM—Part I: Fundamentals and digital CAP transmitter," Contribution to ANSI X3T9.5 TP/PMD Working Group, Minneapolis, MN, USA, Jun. 23, 1992.
[17] G. Stepniak, "Comparison of efficiency of N-dimensional CAP modulations," *J. Lightw. Technol.*, vol. 32, no. 14, pp. 2516–2523, Jul. 2014.
[18] R. Fischer and J. Huber, "A new loading algorithm for discrete tone modulation," in *Proc. GLOBECOM*, 1999, vol. 2, pp. 724–728.
[19] S. Stern and R. Fischer, "Efficient assessment of the instantaneous power distributions of pulse-shaped single-and multi-carrier signals," in *Proc. 1st Int. BlackSeaCom*, 2013, pp. 12–17.